Non-Boussinesq properties of Zonal Flows and GAMs

K. Hallatschek, R. Hager,

Max-Planck-Institut für Plasmaphysik, EURATOM Association, Garching, Germany

Introduction

Geodesic acoustic modes (GAMs) can be a significant agent controlling and modulating the turbulence in the edge. This has been shown by turbulence simulations [1, 2, 3] and possibly recently by experiments [4, 5]. The proximity of the plasma boundary causes the rather short gradient lengths typical for the edge, comparable to the ambient turbulence and GAM scale lengths. Since there is no clear scale separation between fluctuations and background, the background can not be taken as infinitely large and immovable, i.e., the Boussinesq approximation breaks down. This breakdown is described by the local ratio of turbulence to background gradient scale lengths $\lambda^{-1} = L_\perp/L_n \propto \rho^* = \rho_s/R$, with the turbulence scale length $L_\perp$, whereby $\lambda \sim 5-50$ for typical edge scenarios. The rapid change of the parameters – in particular that of the sound speed being proportional to the linear GAM frequency – renders the radial interaction of the GAMs on neighbouring flux surface [6, 7] quite important, and raises the question in what spatial pattern the GAMs will organize themselves. This could involve reflection layers exhibiting a peaking of the GAMs, radial propagation of GAM energy away from turbulent regions generating it, or nonlinear changes of the GAM dispersion relation.

Several different turbulence scenarios have been examined numerically with the NLET code [3] using two-fluid electrostatic Braginskii equations with modified parallel heat conduction coefficient implementing a collisionless heat flux limit. The magnetic geometry was represented for this study by simple $s-\alpha$ geometry.

Slow parameter variation — $\lambda \sim 200$

Fig. 1 shows a typical case of GAMs being excited by high gradient ITG modes in case of still relatively slow parameter variation. From the flow pattern (a) it is obvious that the oscillation frequency decreases towards the edge, which is due to the decreasing sound speed, otherwise apparently rather unaffected by the parameter variation. As is seen in Boussinesq simulations [1], the GAMs are excited with a preferred radial wavenumber, which together with the linear GAM frequency sets the observed inward and outward phase velocities. The Fourier transform of the poloidal flow velocity with respect to time (b) reveals that the frequency depends continuously on the spatial variable. An asymmetry is however conspicuous in the spectrum: there is an amplitude of the GAMs of a particular frequency even at somewhat larger radii than the

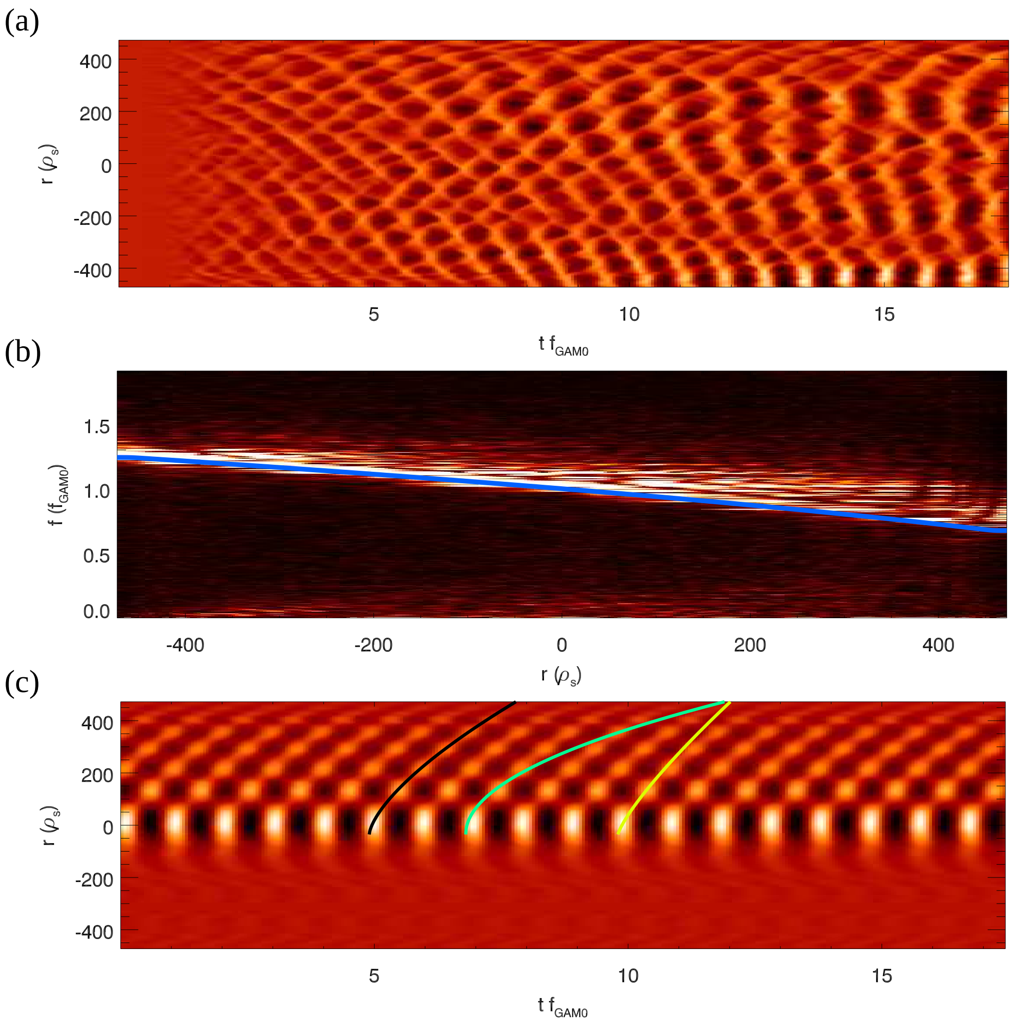

Figure 1: (a) GAM poloidal flow velocity for linear density and temperature profile, $\eta_i = L_n/L_T = 2.4, \varepsilon_n = .05, \alpha_d = 0.5$ (for definitions see [3]). $f_{GAM,0}$ is the GAM frequency at $r = 0$. (b) Radial dependence of frequency spectrum; linear GAM frequency (blue line). Note the GAM activity at $x = 300\rho_s$ at 140% of the linear frequency. (c) Filtered component at $f = 1.02 f_{GAM,0}$; fit with $r(t) = \alpha(t-t_0)^{2/3}$ (black), $r \propto (t-t_0)^{1/2}$ (green), $r \propto (t-t_0)^{4/5}$ (yellow).

one corresponding to their linear frequency (blue line), but not the other way round. The GAMs *radiate outward* from a given radius. The cause for this effect can be gleaned by transforming selectively one frequency of the Fourier representation into real space, as shown in (c). The particular GAM is seen to correspond to a wave travelling inward (to lower radii) and being reflected by the surface corresponding to $k_r = 0$. This can be comfirmed by comparison of the shape of the waves close to the reflection with the one obtained from a generic GAM dispersion relation. We approximate the GAM dispersion relation close to $k_r = 0$ by

$$\omega_{GAM}(r,k_r) = \omega_{GAM}(r,0)(1+\alpha k_r^2) = \gamma c_s(r)(1+\alpha k_r^2), \tag{1}$$

where γ is the geometry dependent ratio of GAM frequency and sound speed and α sets the strength of the dispersion (the linear term has to vanish for symmetry reasons). (As it turns out α is much larger than expected from the linear dispersion.) Since the frequency is fixed in Fig. 1 (b), one obtains from a WKB argument

$$k_r = \sqrt{\left(\frac{\omega_{GAM}}{\gamma c_s(r)} - 1\right)/\alpha} \approx \sqrt{\frac{\partial_r \omega_{GAM}}{\alpha \omega_{GAM}(r_0, 0)}(r_0 - r)}, \tag{2}$$

with cut-off/reflection occuring at r_0 with $\omega_{GAM,0} = \gamma c_s(r_0)$. Any curve $r(t)$ of constant phase has to follow the equation

$$r' \partial_r \phi = \partial_t \phi \Rightarrow r' k_r(r) = \omega_{GAM} \Rightarrow r' \sqrt{(\partial_r \omega_{GAM}/(\alpha \omega_{GAM,0}))(r_0 - r)} = \omega_{GAM} \tag{3}$$

$$\Rightarrow \frac{2}{3}\sqrt{-\partial_r \omega_{GAM}/(\alpha \omega_{GAM,0})}(r(t) - r_0)^{3/2} = \omega_{GAM}(t - t_0) \tag{4}$$

$$\Longleftrightarrow r(t) = r_0 + \left[-\frac{9\alpha \omega_{GAM}^3 (t - t_0)^2}{4\partial_r \omega_{GAM}}\right]^{1/3}. \tag{5}$$

The predicted curve of form $r(t) = r_0 + c(t - t_0)^{2/3}$ has been fitted to one of the wave fronts in (c). A slightly different exponent results already in a misfit, corroborating the correctness of the ansatz (1) for the nonlinear dispersion relation. The dispersion coefficient $\alpha \approx 100\rho_s^2$ extracted from the fit is much larger than expected from linear GAM dispersion relations ($\sim \rho_s^2$) – it is thus a predominantly nonlinear effect. (The sign of α depends on the turbulence parameters. E.g., for higher $\eta_i \sim 5$ and otherwise identical parameters, the reflection scenario of the GAMs turns out to be exactly reversed.) The corresponding *nonlinear* group velocity of the GAMs selected by the turbulence of order $4\rho_s \omega_{GAM}$ is even significantly larger than the maximum curvature drift velocities $v_d \sim \rho_s c_s/R$ which limit the linear group velocity of the GAMs [6, 7]. In other words, the GAM frequency in the presence of turbulence differs from the linear GAM frequency by a factor $1 + \alpha k_r^2$ ($\sim$ 30% here), whereby, owing to the observed reflection layers, the actual k_r will depend also on the radial profile of the sound speed.

Strong parameter variation — $\lambda \leq 50$

For sufficiently strong parameter variation, the GAMs may be generated only in a part of the computational domain, as shown in Fig. 2 for $\lambda = 50$. The GAMs radiate outward from the generation region at $r \sim 0$, maintaining their frequency, which indicates a radial energy transfer. The short radial decay length prohibits the straighforward application of the WKB method. The phase velocity is nevertheless directed outward from the point where the GAMs are generated, i.e., in the direction of the energy flow. The fact that phase velocity and energy flow point in the same direction is again consistent with (1) for positive α. In contrast to the case of weak

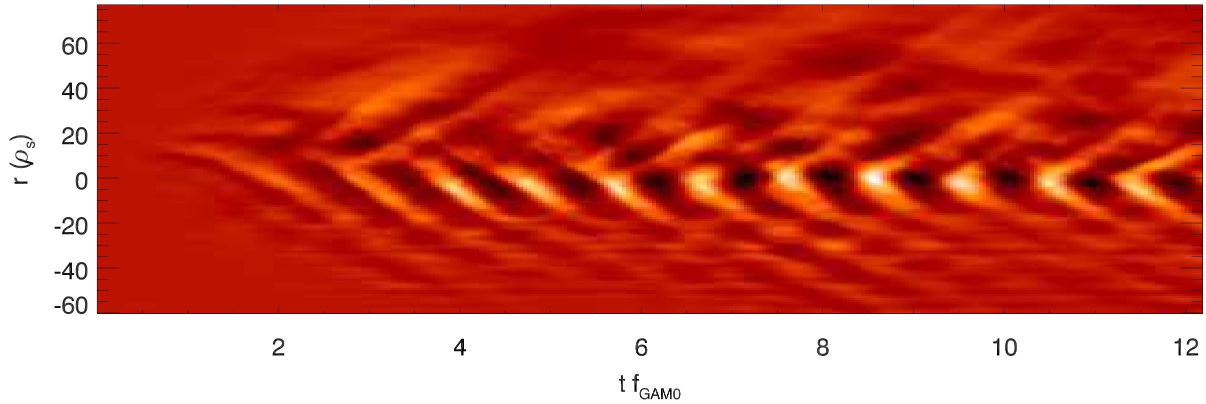

Figure 2: GAM poloidal flow for strong parameter variation. Parameters at center $\lambda = 50, \eta_i = 2.5, \varepsilon_n = 0.3$ (for details see [3] fig. 1b).

parameter variation in the preceding section, the GAMs are damped by the turbulence away from the generation region and can therefore not propagate significant distances.

Summary

In the presence of non-Boussinesq effects, i.e., a significant parameter variation on turbulence scale lengths, the turbulent modifications of the dispersion relation of the GAMs become important, completely dominate linear dispersive effects and greatly increase the radial group velocities. In the case of an extended region of GAM generating turbulence, propagation of the GAMs rather far away from the point of their base frequency can be observed. In the opposite case only a weak propagation into regions where GAMs are damped occurs. The fact that the turbulence nonlinearly modifies the GAM dispersion relation, can lead to the set-up of completely nonlinear reflection and absorption layers. This allows for complex global mode structures, depending on the variation of the turbulence parameters.

References

[1] K. Hallatschek, D. Biskamp, Phys. Rev. Lett. **86**, 1223 (2001)

[2] K. Hallatschek, Plasma Phys. Control. Fusion **49**, B137 (2007)

[3] K. Hallatschek, et al., Phys. Plasmas **7**, 2554 (2000)

[4] R. J. Maqueda, S. J. Zweben, et al., this conference

[5] G. D. Conway, et al., Plasma Phys. Control. Fusion **50**, 055009 (2008)

[6] R. Hager, K. Hallatschek, Phys. Plasmas **16**, 072503 (2009)

[7] R. Hager, K. Hallatschek, Phys. Plasmas **17**, 032112 (2010)